

FIG. 1. Influence of packing on bubble deformation, liquid: silicone oil of viscosity $\nu = 10^3$ cS. (a) Time-series of a compact arrangement of large air bubbles, the symbol * labels a reference bubble as it travels downstream ($\Delta t = 5.5$ ms). (b) Compact and dilute arrangements of small CO_2 bubbles, from top to bottom: decreasing gas volume fraction.

Bubbles in complex microgeometries at large capillary numbers

Martin Sauzade and Thomas Cubaud
*Department of Mechanical Engineering, Stony Brook University, Stony Brook,
 New York 11794, USA*

(Received 7 August 2014; published online 19 September 2014)

[<http://dx.doi.org/10.1063/1.4893544>]

Multiphase flows in confined geometries exhibit a variety of intriguing morphologies. At the small scale, the unique balance of forces produces flow patterns that are typically governed by viscous and capillary effects. While surface tension tends to minimize liquid-gas interfacial areas with bubbles having spherical shape, viscous creeping flows can also strongly deform bubbles in velocity fields set with the channel geometry. Here, the deformation of capillary surfaces is accentuated with the use of a highly viscous carrier fluid (silicone oil having a viscosity $\nu = 10^3$ or 10^4 cS) and the presence of circular cavities along a square microchannel ($h = 250 \mu\text{m}$) for smoothly modulating flow velocity. Although the size and concentration of air bubbles are usually determined through pressure and microfluidic flow rates of injection, the use of carbon dioxide bubbles allows us to manipulate mass transfer processes¹⁻³ (i.e., dissolution and stripping mechanisms) and generate a variety of multiphase flow patterns (Figs. 1 and 2). For instance, as CO_2 bubbles considerably shrink before reaching the field of view, dense arrangements of small bubbles can be produced. In the viscous-dominated regime with a capillary number $\text{Ca} \sim O(1)$, gas bubbles adopt a range of shapes depending on their size and packing. In particular, when passing through a series of extensions and

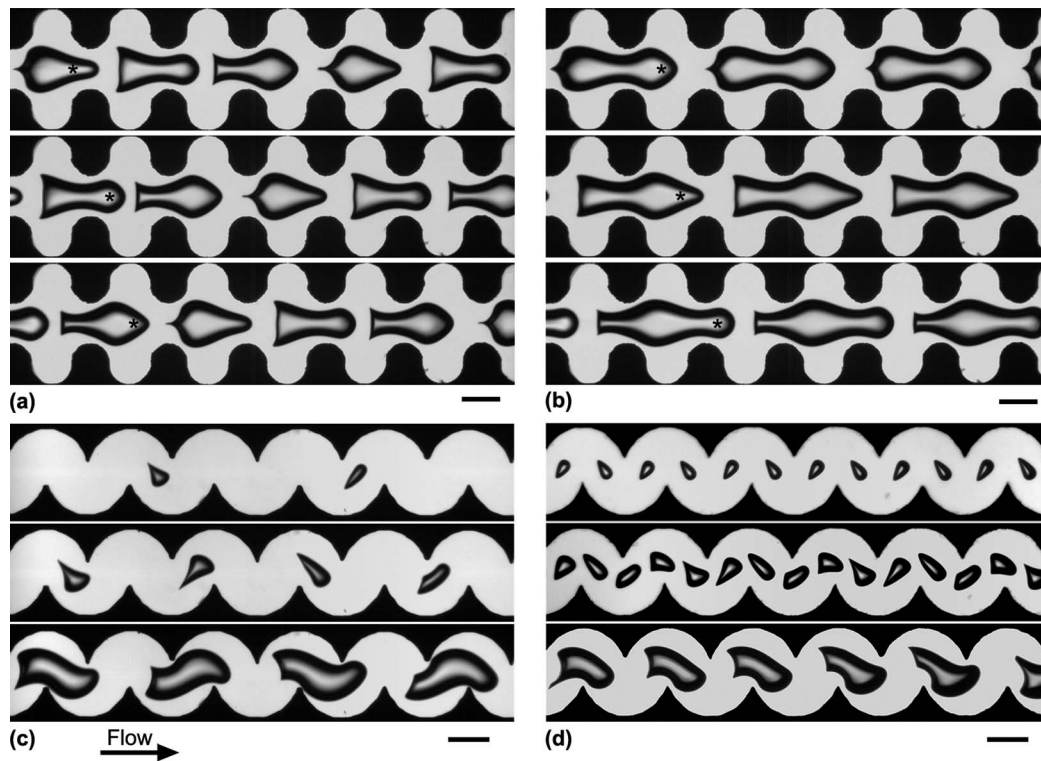


FIG. 2. (a) and (b) Time-series of elongated air bubbles flowing with an oil of viscosity $\nu = 10^3$ cS in a mildly deformed microchannel, the symbol * labels a reference bubble as it travels downstream. Depending on channel geometry and initial liquid-gas flows conditions, various dynamics are observed: (a) bubbles are out of phase ($\Delta t = 2.3$ ms), and (b) bubbles are in phase ($\Delta t = 3.1$ ms). (c) and (d) High-viscosity multiphase flow patterns in a corrugated microchannel, from top to bottom: increasing gas volume fraction, (c) air bubbles with a 10^3 cS-oil, (d) carbon dioxide bubbles with a 10^4 cS-oil. All scale bars: $250 \mu\text{m}$.

constrictions, bubbles are observed to strongly elongate in accelerating flow regions and widen in decelerating flow fields. These experiments illustrate the possibility to control the flow morphology of microbubbles through the interplay between channel geometry, viscous flow, and mass transfer processes.

This material is based upon work supported by the National Science Foundation under Grant No. CBET-1150389.

¹T. Cubaud, M. Sauzade, and R. Sun, "CO₂ dissolution in water using long serpentine microchannels," *Biomicrofluidics* **6**, 022002 (2012).

²M. Sauzade and T. Cubaud, "Initial microfluidic dissolution regime of CO₂ bubbles in viscous oils," *Phys. Rev. E* **88**, 051001(R) (2013).

³S. Shim, J. Wan, S. Hilgenfeldt, P. D. Panchal, and H. A. Stone, "Dissolution without disappearing: Multicomponent gas exchange for CO₂ bubbles in a microfluidic channel," *Lab Chip* **14**, 2428 (2014).